The Curious Case of the Hottest (and Coldest) FOVs

dave.tobin@ssec.wisc.edu

David Tobin[1], Chris Barnet[2], John Blaisdell[3], Liam Gumley[1], Robert Knuteson[1], Willem Marais[1], Graeme Martin[1], Hank Revercomb[1], Joe Taylor[1]

[1]Space Science and Engineering Center, University of Wisconsin – Madison, Madison, WI, 53706

[2]Science and Technology Corp, Columbia, MD 21046

[3]Science Applications International Corporation, Reston, VA 20190

ITSC-23
24-30 June 2021
Poster 4p.17

OBSERVATIONS

The Cross-track Infrared Sounder (CrIS) collects radiance spectra in three spectral bands each with a 3x3 detector array. For each Field-of-Regard (FOR), each detector corresponds to an Earth view Field-of-View (FOV), with the FOVs labelled 1 through 9, as shown in the scan pattern from Han et al. The CrIS calibration process is tailored to produce radiance data with high accuracy and low noise and also to minimize FOV-to-FOV biases so that data from the different FOVs can be used interchangeably.

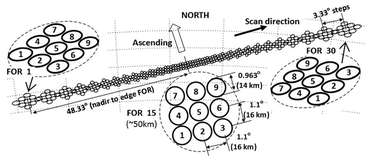

The following is a series of example analyses of CrIS, VIIRS, AIRS, and digital photo data …

A) Using one day of NOAA-20 CrIS radiance data (7 June 2020), for each of the 324,000 FORs, the hottest and coldest FOVs are recorded*. This is done using the Longwave band radiance data. The percentages of which FOVs observe the hottest and coldest radiance values are:

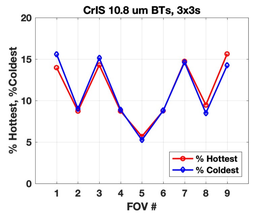

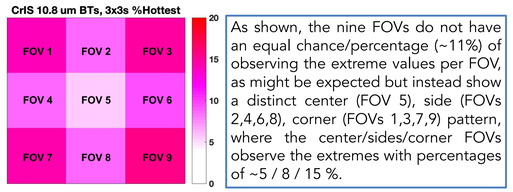

As shown, the nine FOVs do not have an equal chance/percentage (~11%) of observing the extreme values per FOV, as might be expected but instead show a distinct center (FOV 5), side (FOVs 2,4,6,8), corner (FOVs 1,3,7,9) pattern, where the center/sides/corner FOVs observe the extremes with percentages of ~5 / 8 / 15 %.

This type of behavior was first noted by Wolf et al. in 2005, where AIRS footprints were arranged into 3x3 array "golfballs" for the purpose of cloud clearing and atmospheric sounding. More recently in terms of CrIS "pre-screening" or thinning procedures for Data Assimilation, this behavior was noted in 2017 by Jung et al. and by Eresmaa et al.

B) VIIRS radiance and Cloud Mask data collocated within the CrIS footprints is provided in the CrIS/VIIRS IMG product (Revercomb and Strow, 2020). Using the mean all-sky VIIRS radiance values within each CrIS footprint, the same hottest/coldest FOV analysis was performed on the 7 June 2020 data. Additionally, using the VIIRS cloud mask data within each CrIS footprint, the percentages of clearest and cloudiest FOVs were compiled, and the results are:

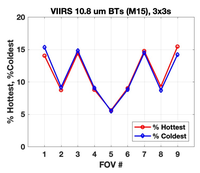

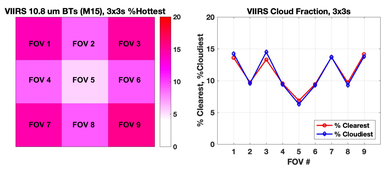

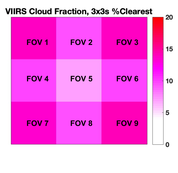

C) AIRS data (which natively provides a single FOV per FOR), from 6 Nov 2019 was arranged into 2x2, 3x3, 4x4, and 5x5 footprint arrays, and analyzed in the same way:

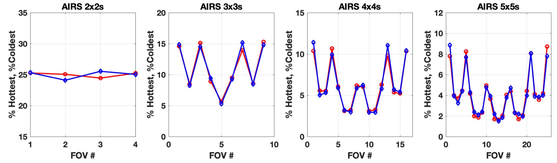

(Also noted but not shown is the dependence of these probabilities on view angle due to the increase in FOV size with increasing view angle and for CrIS also the FOR rotation.)

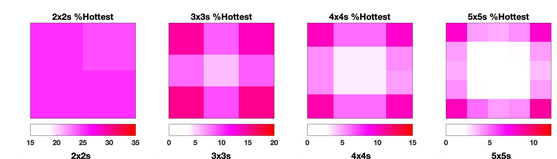

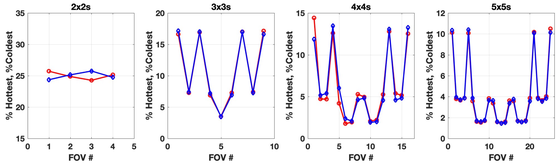

D) Finally, a digital photograph, the red component of the ITSC-22 group photo, was also analyzed the same way:

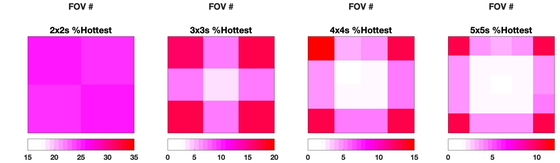

*Infrequent ties (of values from N FOVs within the FOR) are broken through a process of random selection to arrive at one value/FOV to represent that set (of ties), repeating the process for each tie.

SUMMARY

When clustered into NxN (with N>2) arrays (FORs) of FOVs, satellite and other image type data display the behavior that the hottest and coldest extreme values do not occur with equal probability for all FOVs, but occur most frequently for the corner FOVs, followed by the side FOVs, and central interior FOVs having the same but lowest probability of observing the extremes.

This is observed to be a pervasive yet often unrecognized and/or misunderstood feature of imagery, which is due to the analysis of relative and finite clustered data combined with an underlying structured scene. The effect occurs even though the probability distribution functions for each FOV for the full data set are all equal!

This behavior can be explained, with varying assumptions, with both analytical solutions and simulations. Simulations assuming large spatial scale boundaries or gradients, and simulations of randomly placed small scale features do a good job of representing the observed behavior, with both effects contributing depending on the specific scenes considered.

Various satellite data analysis and processes utilize FOV clustering and contrast within a FOR, such as cloud clearing to estimate clear sky radiance spectra, climate studies using selected hottest and/or coldest data subsets, and data thinning for NWP data assimilation. Determining the implications, if any, of this hottest/coldest FOV phenomenon on those applications, is the topic of on-going investigations.

EXPLANATIONS

The hottest/coldest FOV (or pixel) phenomenon is observed for CrIS data, VIIRS data, AIRS data, and other sources of satellite data, as well as for the majority of other image types such as digital photographs of people and landscapes. The phenomenon is not due to underlying calibration biases of individual FOVs or FOV-to-FOV biases (although, if large enough, FOV-to-FOV calibration biases could mask the hottest FOV behavior). It is also not due to systematic differences in view angle differences between the FOVs. The phenomenon is found to not occur for a few special cases, such as entirely "flat" fields all of the same values, or images consisting of entirely random and spatially uncorrelated values.

Qualitatively, for Earth view satellite data, the center FOVs are less likely to observe the extremes due to the relatively infrequent cases where, for example, a cloud primarily impacts the center FOV without impacting the surrounding side and corner FOVs, while there are more cases, both in terms of cloud size and orientation, that can impact the side and corner FOVs. In other words, for a cloud to impact only the center FOV it would need to be small enough and also placed perfectly in the center of the FOR. However, this phenomenon is not due solely to clouds, as the same behavior is seen for ensembles of clear sky spectra, and for other independent imagery. Another qualitative reasoning is that the corner FOVs have the least number of adjacent neighbors, side FOVs have more neighbors, and center FOVs have the most neighbors. For the case of 2x2 FORs (e.g. IASI), all FOVs have the same number of neighbors and this behavior is not observed.

Examples of quantitative explanations of the observed behavior are:

Calculations using straight line boundaries with warm on one side, cold on the other

Consider 3x3 FOV FORs, and the relatively simple case of large, straight line boundaries across the FOR where it is warm on one side of the boundary and cold on the other side. But first consider the one dimensional case, with a row of three slits, and the division can equally fall in any of the slits:

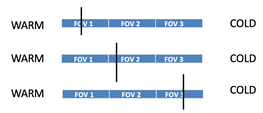

In the first two cases FOV 1 is the warmest, and in the third case FOV 1 and FOV 2 tie, so we will give them equal likelihood in the third case. These cases sum to award FOV 1 with 5/6 probability and FOV 2 with 1/6 probability. It is equally likely that the WARM scene could be to the right, and in those cases FOV 3 is warmest with probability 5/6 and FOV 2 with probability 1/6. Combining these, we see the distribution is: 5/12, 1/6, 5/12. Already we see how the uniqueness of the end position is favored.

For a 3x3 array of FOVs, adjacent square FOVs are used for ease of computation. The computation is an exercise in geometry to count all the ways that a single straight line can intersect the FOR, dividing it into warm and cold scenes. The details of the computation are not included here, but provide probabilities of observing the extremes as shown below. This simplified case comes surprisingly close to the observed distribution. Clearly features of smaller size do exist and must be considered, but this result strengthens the intuition of the observed behavior.

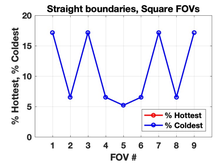

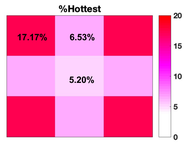

Calculations using randomly shaped and placed polygons and using VIIRS I-band data

For smaller scale features, the simulation of small hot/cold features was performed using square features and 3x3 square FOVs. The corner/side/center probabilities as a function of the relative feature FOV size can be solved analytically:

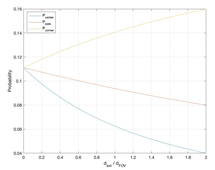

$$P_{center} = \frac{d_{FOV}^2}{L^2}$$

$$P_{side} = P_{center} + 2\frac{\frac{1}{2}d_{FOV}d_{sf}}{L^2}$$

$$P_{corner} = P_{center} + \frac{d_{FOV}d_{sf} + \frac{1}{4}d_{sf}^2}{L^2}$$

$$L = 3d_{FOV} + d_{sf}$$

Simulations were also performed with VIIRS I-band (375 m) data, and with underlying purely random data, for 3x3 arrays of 14 km circular FOVs. In each case the spatial resolution of the underlying scene is reduced in resolution from the original high resolution, before being sampled by the 14 km FOVs:

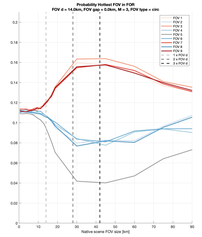

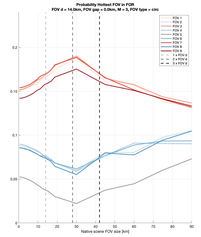

These simulations demonstrate the dependence of the effect on the scale/resolution of the underlying structured, or random, scene.

IMPLICATIONS ?

Example applications which utilize the analysis of clustered data within a FOR include: "cloud clearing" which utilizes the contrast of FOVs within the FOR to estimate a clear sky spectrum for atmospheric sounding, the selection of spatially uniform FORs based on the variability of radiance values within a FOR, the selection of hottest or coldest FOVs per FOR for climate trending, and the pre-screening or selection of warmest FOVs within a FOR for NWP data assimilation.

A curious and perhaps non-intuitive observation is that the underlying distributions of radiances from each FOV do not differ from one another in order to observe this phenomenon, even though corner and side are more likely to be warmer (and colder) than the center FOV. This can be demonstrated by performing an alternate analysis where the 3x3 FOV FORs are offset by 1 row and 1 column and performing the same analysis. In this case the previously labelled center FOV is now a corner, and a previously labeled corner FOV is now the center, and yet the same FOV pattern is observed. This is also demonstrated with the following Thought Experiment /proof:

Thought experiment that highlights the perversity of interpreting the implications:

1. The probability of getting the hottest or coldest from say the corner or center of a 3x3, if only those two FOVs are compared will be 50% (a demonstration of this for CrIS 3x3s and only comparing FOVs 1 and 5 is shown below)
2. The same result is found for any other two FOVs.
3. This proves that the extremes of the radiance PDFs for all FOVs are equal.

(So, why favor picking any specific subset of FOVs?)

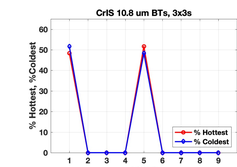

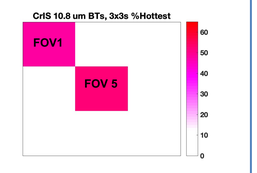

The hottest FOV (per FOR) behavior is therefore observed, even though this does not require there to be differences in the distribution functions of radiances from the individual FOVs. Here is an example study, where for one day's worth of CrIS data, the warmest FOV per FOR is determined considering all nine FOVs, versus when only the side FOVs are considered. In this case, differences in the warmest-value-per-FOV can be as large as 30 to 40 K even for warm scenes. However, for scenes with BT greater than 280K, only 10 percent of the FORs have BT differences of 1K or more.

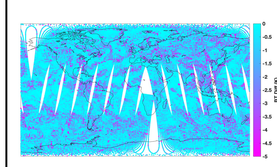

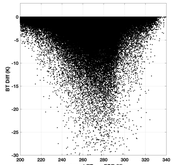

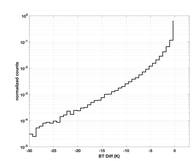

REFERENCES

Han, Y., et al. (2013), Suomi NPP CrIS measurements, sensor data record algorithm, calibration and validation activities, and record data quality, J. Geophys. Res. Atmos., 118, 12,734– 12,748.

Walter Wolf, T. King, L. Zhou, M. Goldberg, C. Barnet, R. Holz, NOAA Near Real-Time AIRS Processing System: Using MODIS with AIRS, SPIE Conference, San Diego, CA, 2005.

James Jung, A. Collard, K. Bathmann, D. Groff, A. Heidinger, M. Goldberg, Preparing for CrIS Full Spectral Resolution Radiances in the NCEP Global Forecast System, ITSC-21, 2017.

Reima Eresmaa, J, Letertre-Danczak, C. Lupu, N. Bormann and A. P. McNally, The assimilation of Cross-track Infrared Sounder radiances at ECMWF, Q. J. R. Meteorol. Soc. 143: 3177–3188, October 2017

Henry Revercomb and L. Strow (2020), S-NPP CrIS IMG: Collocated VIIRS level 1 / cloud mask statistical summary V2, Greenbelt, MD, Goddard Earth Sciences Data and Information Services Center (GES DISC)